

# Immobilization of Enzymes in Porous Solids Under Restricted Diffusion Conditions

A restricted diffusion model is developed to study the immobilization of enzyme in porous solid supports. Simulation studies have been carried out for various combinations of process variables and parameters of the immobilization system. The model has also been used to develop a method for estimating the intrinsic rate constant of immobilization when enzyme diffusion into the support is restricted. Results of experiments in which glucose oxidase was immobilized in porous glass supports are consistent with model simulations.

**Md. M. Hossain and D. D. Do**  
Department of Chemical Engineering  
University of Queensland  
St. Lucia, Qld. 4067, Australia

**J. E. Bailey**  
Department of Chemical Engineering  
California Institute of Technology  
Pasadena, CA 91125

## SCOPE

One of the most interesting recent developments in applied catalysis is the increase in knowledge of methods for immobilizing enzymes. Chemical coupling of enzymes with porous supports is frequently used for immobilization because of the high surface area available for coupling (thus high activity). This process involves diffusion of free enzyme within pores and surface attachment of enzyme. Restricted diffusion arises when the enzyme molecular size is comparable to the pore size of the support. Reduced enzyme diffusion fluxes occur under these conditions because the enzyme is excluded from an annular region adjacent to the pore wall, and because hydrodynamic resistance

hinders enzyme movement into the pores. A restricted diffusion model has been developed based on coupled restricted diffusion and immobilization processes. Analysis and simulations based on this mathematical model will help in the interpretation of immobilization experiments when enzyme diffusion is restricted, and will help in improving the ultimate characteristics of the immobilized enzyme catalyst. Computer solutions have been developed that permit evaluation of the influences of different immobilization process variables and different degrees of restriction. Model solutions have been compared to experimental data from immobilization of glucose oxidase in porous glass particles.

## CONCLUSIONS AND SIGNIFICANCE

The mathematical model and the computer solutions presented characterize the effects of enzyme restricted diffusion on immobilization time and on spatial distribution of enzyme loading inside the porous support for various controlling regimes and for different degrees of restriction to diffusing molecules. The enzyme loading profile is uniform when the system is kinetic-controlled. When the Thiele modulus is larger, progressively more nonuniform profiles are obtained. For very large values of Thiele modulus, the transient profile is very sharp and behaves like a wave front. Consequently, by properly choosing experimental vari-

ables and carrying out the immobilization for a short period of time, we can load the enzymes near the external surface. This outer-shell-immobilized enzyme in many cases will yield higher activity than the uniformly distributed enzyme for the same amount of enzyme loaded.

The restricted diffusion model fits experimental results for glucose oxidase in porous glass better than the unrestricted counterpart. The model solution provides a basis for analysis of the experimental data to compute the intrinsic rate constant for binding of enzyme onto the internal surfaces of porous support. The present model may be used to manipulate immobilization variables or parameters to obtain a desired enzyme loading profile.

Correspondence concerning this paper should be addressed to D. D. Do.

## Introduction

Enzymes have been immobilized onto a wide range of porous supports by either physical or chemical techniques. Immobilized enzymes are prepared by contacting the porous solid, after chemical pretreatment, with enzyme solutions. During this process, enzyme diffuses into the solid matrix and attaches onto the internal surfaces of the support. The final spatial distribution of immobilized enzyme within the support particles depends on the variables and parameters that characterize the complex transport and immobilization processes during catalyst preparation.

The situation becomes more complex when the enzyme molecular size is comparable to the pore size of the support. This is due to the phenomenon called restricted or hindered diffusion. The restriction is caused by the solute's being excluded from a fraction of the pore volume leading to equilibrium partitioning, and by the hydrodynamic resistance hindering the movement of solute molecules through the pore. Restricted diffusion is observed in heterogeneous catalysis, gel permeation chromatography, membrane dialysis, and separation processes.

Pappenheimer et al. (1951) were the first to point out the above phenomenological concepts. Their analysis was improved by Renkin (1954) to accommodate higher degrees of restriction. The combined model equation proposed by Renkin is:

$$\frac{D_e}{D_b} = \left(1 - \frac{a}{R_p}\right)^2 \left[1 - 2.104 \left(\frac{a}{R_p}\right) + 2.09 \left(\frac{a}{R_p}\right)^3 - 0.95 \left(\frac{a}{R_p}\right)^5\right] \quad (1)$$

Several theoretical models of diffusion in fine pores have been developed based on either a hydrodynamic approach or on scaling arguments for polymeric molecules. Hydrodynamic theories of mass transfer have been applied to the transport processes across synthetic and biological membranes (Beck and Schultz, 1972; Malone and Anderson, 1977; Deen et al., 1981; Bohrer et al., 1984), diffusion in pores of silica-alumina (Satterfield et al., 1973), and diffusion in porous glass (Colton et al., 1975). Useful statistical and hydrodynamic principles of the development of these theories are discussed by Bean (1972), Anderson and Quinn (1974), Brenner and Gaydos (1977), Malone and Anderson (1978), and Klein et al. (1979). In general, the theories are based on the following assumptions:

- The diffusing molecule is a rigid sphere and larger than the molecules of the solvent.
- The porous medium is modeled as an array of identical cylindrical pores.
- The solute is assumed to have both Brownian and hydrodynamic characteristics and the solvent is a continuum.
- The pore wall is smooth and the length/diameter ratio of the pore is large.
- There are no particle-particle interactions.

All the equations derived for hindered diffusion of uncharged spheres adequately approximate the Renkin model, which actually is reasonably accurate over the entire range  $0 \leq a/R_p \leq 0.4$  (Malone and Anderson, 1978).

A second approach to modeling hindered diffusion is based on the scaling theory arguments presented by de Gennes (1979). Daoud and de Gennes (1977) have investigated equilibrium partitioning, and Brochard and de Gennes (1977) have treated the

diffusion of polymers in porous media. All the results have been combined by Cannell and Rondelez (1980) to examine the effects of the degree of restriction on  $D_e/D_b$ ; the result is

$$\frac{D_e}{D_b} = \gamma \{\beta \alpha^{-2/3} \exp [-(\beta \alpha)^{5/3}]\} \quad (2)$$

where  $\gamma$  and  $\beta$  are proportionality constants. However, this approach predicts only the power law behavior for the diffusion and partitioning and does not give exact numerical coefficients.

In order to understand the interaction of different process variables and parameters on the immobilization process under restricted diffusion conditions, a mathematical model taking into account the restricted diffusion of enzymes within pores is necessary.

Carleysmith et al. (1980) have developed a model for enzyme adsorption under a diffusion-controlled situation and have observed nonuniform internal profiles experimentally. The model proposed by Do et al. (1982b) also predicts nonuniform profiles when the diffusion rate is comparable or slower than the surface coupling rate. However, that model did not consider the effect of the size of the macromolecules in their diffusion and immobilization; consequently, it does not apply to the restricted diffusion conditions that are expected in many practical immobilization processes.

Recently it was suggested by Dennis et al. (1984) that restricted diffusion may cause nonuniform distribution of enzymes in porous supports. On the basis of this, a mathematical model has been formulated by Clark et al. (1985). Although they have taken into account restricted diffusion effects, their model is incomplete because the time-varying bulk enzyme concentration is not considered. So they suggested that this situation should be incorporated in the model (as it exists in practice) to calculate the amount and the internal distribution of enzymes for real processes.

In the present study, a restricted diffusion model is developed with time-varying reservoir enzyme concentrations and solved for various combinations of physicochemical parameters and operating variables. An approximate analytical solution is obtained for the initial period of the immobilization process in which the surface contains an insignificant amount of immobilized enzymes. This simple solution allows quick determination of the intrinsic immobilization rate constant. The solutions of the complete model equations are able to predict the spatial distribution of the immobilized enzyme within the bed. Such knowledge will help in the quantitative design of enzyme supports and immobilization processes.

## Problem Formulation

Consider an isothermal process in which enzyme is immobilized in porous solid supports, the pore size of which is comparable to the diameter of the enzyme molecules. The immobilization process is carried out in a batch reactor. The enzyme-free particles, after chemical treatment, are immersed in a well-mixed bath of enzyme solution with initial concentration  $e_{b0}$ . The physical realization of this situation is a fixed-bed, closed recirculation system with low loading per pass so that it behaves as a well-mixed batch reactor. The following assumptions are made for the modeling of enzyme immobilization with restricted entry to the supports.

1. The porous support particles are spherical with pore size comparable to that of enzyme molecule.

2. The pores are initially filled with buffer so that there is no fluid convection into the particles when the immobilization process is initiated.

3. Enzyme molecules are transported from the bulk immobilizing solution to the exterior surface of the particles (mass transfer coefficient), where they start to diffuse into the particle. The effective diffusion coefficient  $D_e$  is a function of the local enzyme loading.

4. It is assumed that the enzymes attach only to the pore interior surfaces that contain a uniform distribution of functional groups.

5. The rate of enzyme immobilization per unit interior surface area for irreversible covalent coupling used is (Do et al. 1982b)

$$V_{im} = k_{im}e(r) \left[ 1 - \frac{e_s(r)}{e_{sm}} \right], \quad (3)$$

where  $k_{im}$  is the rate constant per unit available surface area,  $e(r)$  is the pore fluid enzyme concentration based on effective pore volume,  $e_s(r)$  is the immobilized enzyme concentration, and  $e_{sm}$  is the support's maximum capacity for immobilization, having dimensions of mass of enzyme per unit mass of support.

6. For intraparticle diffusion, Fick's law holds with the effective diffusion coefficient  $D_e(r)$  defined as

$$D_e(r) = \frac{D_b \epsilon(r) K_p(r) K_r(r)}{\tau} \quad (4)$$

where  $D_b$  is the bulk diffusion coefficient for enzyme,  $\epsilon$  is the particle void fraction,  $K_r$  is the fractional reduction in diffusivity within the pores, and  $\tau$  is the tortuosity factor. The bulk diffusivity for enzyme has been estimated from the formula (Young et al., 1980)

$$D_b = 8.34 \times 10^{-8} (T/\nu M_w^{1/3}) \quad (5)$$

where  $T$  is the absolute temperature in K,  $\nu$  is viscosity in centipoise, and  $M_w$  is the molecular weight of enzyme.

The following equation for  $K_r$ , proposed by Renkin (1954), will be used

$$K_r(r) = \left[ 1 - 2.104 \left( \frac{a}{R_{eff}} \right) + 2.09 \left( \frac{a}{R_{eff}} \right)^3 - 0.95 \left( \frac{a}{R_{eff}} \right)^5 \right], \quad (6)$$

where  $a$  is the radius of the enzyme molecule and  $R_{eff}$  is the effective pore radius of the support particle. This pore radius is a function of the local enzyme concentration and is related to the initial radius by the following approximation

$$R_{eff} = R_p \left[ (1 - E_s) + \left( 1 - \frac{2a}{R_p} \right)^2 E_s \right]^{1/2}, \quad (7)$$

where  $R_p$  is the initial pore radius and  $E_s$  is the nondimensional immobilized enzyme concentration. The porosity of the particle

at any loading can be approximated by the equation:

$$\epsilon(r) = \left[ \left( 1 - \frac{e_s}{e_{sm}} \right) + \left( 1 - \frac{2a}{R_p} \right)^2 \frac{e_s}{e_{sm}} \right] \epsilon_0 \quad (8)$$

This has been derived assuming immobilized enzyme surface coverage is at most monolayer and the void spaces in the particle may be approximated as cylindrical pores with uniform cross section. The derivations are available in Hossain (1985). For  $K_p$  the following formula proposed by Ferry (1936) is used

$$K_p(r) = \left[ 1 - \frac{a}{R_{eff}|_{r_p}} \right]^2 \quad (9)$$

where  $R_{eff}|_{r_p}$  is evaluated at the particle surface.

## Formulation of the Mathematical Model

**Intraparticle Material Balance.** Making a material balance on a spherical shell of thickness  $\Delta r$  at a radial distance  $r$  from the center of the pellet and proceeding with standard manipulations gives the following equation describing the enzyme in the particle pore spaces:

$$\frac{1}{r^2} \frac{\partial}{\partial r} \left( r^2 D_e \frac{\partial e}{\partial r} \right) - k_{im} S_g \rho_p e \left( 1 - \frac{e_s}{e_{sm}} \right) = \frac{\partial}{\partial t'} (\epsilon K_p e) \quad (10)$$

**Immobilized Enzyme Material Balance.** The rate of attachment of enzyme per unit mass of support is given by

$$\frac{\partial e_s}{\partial t'} = k_{im} S_g e \left( 1 - \frac{e_s}{e_{sm}} \right) \quad (11)$$

**Reservoir Enzyme Material Balance.** For the batch immobilization process considered, the rate of change of enzyme concentration in the immobilizing solution is equal to the diffusion flux of enzyme into the particles

$$V_b \frac{de_b}{dt'} = - \left( \frac{m_p}{\rho_p} \right) \left( \frac{3}{r_p} \right) \left( D_e \frac{\partial e}{\partial r} \right) \bigg|_{r_p}, \quad (12)$$

where  $e_b$  is the reservoir enzyme concentration and  $V_b$  is the reservoir volume.

The initial and boundary conditions for the model equations are:

$$t' = 0; \quad e_b = e_{bo}, \quad e_s = e = 0 \quad (13)$$

$$r = 0; \quad \frac{\partial e}{\partial r} = 0, \quad (14)$$

$$r = r_p; \quad D_e \frac{\partial e}{\partial r} \bigg|_{r_p} = k_m (e_b - e|_{r_p}) \quad (15)$$

where  $k_m$  is the mass transfer coefficient based on exterior surface area, and calculated from the correlation of Ohashi et al. (1981):

$$Sh = \frac{k_m d_p}{D_b} = 2.0 + 0.51 (\kappa^{1/3} d_p^{4/3} / \nu)^{0.57} (Sc)^{1/3}, \quad (16)$$

where  $Sh$  is the Sherwood number and  $Sc$  is the Schmidt number.

To study the effects of parameters on the immobilization process, we need to nondimensionalize the model equations along with the initial and boundary conditions. This is done by defining the following nondimensional variables and parameters.

$$E_s = \frac{e_s}{e_{sm}}, \quad E_b = \frac{e_b}{e_{bo}}, \quad E = \frac{e}{e_{bo}},$$

$$\beta = \frac{K_p}{(K_p)_{t=\epsilon_0}}, \quad \lambda = \frac{\epsilon K_{po}}{\epsilon_0} \quad (17a)$$

$$x = r/r_p, \quad \psi = \frac{\epsilon_0 e_{bo}}{e_{sm} \rho_p}, \quad t = \frac{(D_e)_{t=\epsilon_0} t'}{r_p^2 \epsilon_0}, \quad (17b)$$

$$Bi = \frac{k_m r_p}{(D_e)_{t=\epsilon_0}}, \quad N = \frac{3(m_p/\rho_p)\epsilon_0}{V_b}, \quad \phi^2 = \frac{r_p^2 S_g k_{im} \rho_p}{(D_e)_{t=\epsilon_0}} \quad (17c)$$

where  $\phi$  is the Thiele modulus, and  $Bi$  is the Biot number. It is noted that the initial porosity and initial effective diffusivity have been used in the nondimensionalization process.

The parameter  $\phi^2$  characterizes the ratio of a characteristic immobilization rate to a characteristic diffusion rate, and the parameter  $Bi$  is a characteristic external mass transfer rate divided by a characteristic diffusion rate. The parameter  $\psi$  gives the ratio of pore fluid enzyme concentration to the maximum possible immobilized enzyme concentration.

The model equations in nondimensional form are:

$$\frac{\partial(E\lambda\beta)}{\partial t} = \frac{1}{x^2} \frac{\partial}{\partial x} \left[ x^2 f_1(E_s) \frac{\partial E}{\partial x} \right] - \phi^2 E(1 - E_s), \quad (18)$$

$$f_1(E_s) = \left[ (1 - E_s) + \left( 1 - \frac{2a}{r_p} \right)^2 E_s \right] \left( \frac{K_r}{K_{ro}} \right) \left( \frac{K_p}{K_{po}} \right), \quad (19)$$

$$\frac{dE_b}{dt} = -N \left[ f_1(E_s) \frac{\partial E}{\partial x} \right]_{x=1}, \quad (20)$$

$$\frac{\partial E_s}{\partial t} = \phi^2 \psi E(1 - E_s), \quad (21)$$

where  $K_{ro}$  and  $K_{po}$  are the initial values of  $K_r$  and  $K_p$ , respectively. The function  $f_1(E_s)$  describes the accentuation of diffusional restrictions during immobilization due to the accumulation of immobilized enzyme on the pore walls of the support. The initial and boundary conditions in nondimensional form are:

$$t = 0; \quad E = E_s = 0, \quad E_b = 1, \quad (22)$$

$$x = 0; \quad \frac{\partial E}{\partial x} = 0, \quad (23)$$

$$x = 1; \quad \frac{\partial E}{\partial x} = \frac{Bi}{f_1(E_s|_1)} [E_b - E|_1], \quad (24)$$

### Initial stage analysis

The mathematical formulation is slightly simpler for the initial stage of immobilization during which the immobilized

enzyme concentration  $e_s$  is much smaller than its maximum concentration  $e_{sm}$ . During this stage, the support acts as an infinite sink for enzyme uptake. The model equations are linear and susceptible to linear analysis. The immobilization rate expression during the initial immobilization interval is:

$$V_{im} = k_{im} e \quad (25)$$

Therefore the nondimensional model equations in the initial stage are:

$$K_{po} \frac{\partial E}{\partial t} = \frac{1}{x^2} \frac{\partial}{\partial x} \left( x^2 \frac{\partial E}{\partial x} \right) - \phi^2 E \quad (26)$$

$$\frac{dE_b}{dt} = -N \frac{\partial E}{\partial x} \Big|_{x=1} \quad (27)$$

$$\frac{\partial E_s}{\partial t} = \phi^2 \psi E \quad (28)$$

The initial and boundary conditions are the same as Eqs. 22–24 with  $f_1(E_s) = 1$ .

In the case of a fast immobilization rate compared to the diffusion rate ( $\phi \gg 1$ ), singular perturbation can be applied to solve the model equations. The solutions are (Do and Bailey, 1981),

$$E_b = \exp \left[ -\frac{N\phi t}{1 + (\phi/Bi)} \right], \quad (29)$$

$$E = \frac{E_b \exp [-\phi(1-x)]}{[1 + \phi/Bi]}. \quad (30)$$

Hence, it can be seen that  $\phi$  and then the immobilization rate constant  $k_{im}$  can be determined immediately from measurements of  $E_b$  vs. time (Do and Bailey, 1981).

### Long time immobilization

In most cases of enzyme immobilization,  $\psi$ , which characterizes the pore fluid enzyme concentration in the support relative to the maximum possible immobilized enzyme concentration, is small. Therefore, the quasisteady state hypothesis is applicable. For long time solution of immobilization processes, the slow time scale is defined as

$$\tilde{t} = \psi t \quad (31)$$

With respect to this time scale, Eqs. 18, 20, and 21 become:

$$0 = \frac{1}{x^2} \frac{\partial}{\partial x} \left[ x^2 f_1(E_s) \frac{\partial E}{\partial x} \right] - \phi^2 E(1 - E_s), \quad (32)$$

$$\frac{dE_b}{d\tilde{t}} = -\left( \frac{N}{\psi} \right) \left[ f_1(E_s) \frac{\partial E}{\partial x} \right]_1, \quad (33)$$

$$\frac{\partial E_s}{\partial \tilde{t}} = \phi^2 E(1 - E_s), \quad (34)$$

in which we have applied the quasisteady state hypothesis. The above model equations along with the initial and boundary con-

ditions, Eqs. 22–24, can be solved by using a combination of the orthogonal collocation technique (Villadsen and Michelsen, 1978) and the Runge-Kutta technique. An effective computational algorithm has been developed (Hossain, 1985) to obtain numerical solutions of the above model equations.

### Analytical asymptotic solutions ( $\phi \gg 1$ )

In this section, solutions are provided for the diffusion-controlled regime ( $\phi \gg 1$ ). The numerical solutions presented earlier require a significant amount of computer time to obtain the simulation results under this condition. Here we employ a powerful tool of matched asymptotic expansions (Cole, 1968; Nayfeh, 1973) to solve the model equations 18–24. According to previous theoretical work of Do and Weiland (1981) and Do et al. (1982a) the time scale  $t$  is too fast to observe any change in the pore fluid enzyme concentration inside the particle. Therefore, to observe the evolution of immobilized enzyme loading we define a slower time scale as in Eq. 31.

With respect to the slow time scale, Eq. 31, Eqs. 18, 20, and 21 become:

$$\psi \mu^2 \frac{\partial(E\lambda\beta)}{\partial \tilde{t}} = \mu^2 \frac{1}{x^2} \frac{\partial}{\partial x} \left[ x^2 f_1(E_s) \frac{\partial E}{\partial x} \right] - E(1 - E_s), \quad (35)$$

$$\frac{dE_b}{d\tilde{t}} = -\sigma \left[ f_1(E_s) \frac{\partial E}{\partial x} \right]_1, \quad (36)$$

$$\mu^2 \frac{\partial E_s}{\partial \tilde{t}} = E(1 - E_s) \quad (37)$$

where

$$\mu^2 = 1/\phi^2 \ll 1, \quad \text{and} \quad \sigma = (N/\psi) \equiv 0(1). \quad (38)$$

The dependent variables are assumed to have the following asymptotic expansions:

$$E = E_o + \mu^2 E_1 + o(\mu^2), \quad (39a)$$

$$E_s = E_{so} + \mu^2 E_{s1} + o(\mu^2), \quad (39b)$$

and

$$E_b = E_{bo} + o(1). \quad (39c)$$

Substitution of these expansions into Eqs. 35–37 and applying the usual perturbation procedure yields the following subproblems:

$0(1)$ :

$$E_o(1 - E_{so}) = 0, \quad (40a)$$

$$\frac{dE_{bo}}{d\tilde{t}} = -\sigma f_1(E_{so}) \left. \frac{\partial E_o}{\partial x} \right|_1, \quad (40b)$$

$0(\mu^2)$ :

$$\frac{1}{x^2} \frac{\partial}{\partial x} \left[ x^2 f_1(E_{so}) \frac{\partial E}{\partial x} \right] - E_1(1 - E_{so}) + E_o E_{s1} = 0, \quad (41a)$$

$$\frac{\partial E_{so}}{\partial \tilde{t}} = E_1(1 - E_{so}) - E_o E_{s1}. \quad (41b)$$

Investigation of Eq. 40a reveals that two solutions are possible, which is consistent with our physical intuition that the spatial domain of porous support is divided into two zones. In one zone, no enzyme is observed, and in the other solid support is saturated with immobilized enzyme.

In the first zone,  $I_1 \equiv [0, X]$ , where  $X$  is the demarcation point between the two zones (and is called later the immobilization front), the solutions are readily found as

$$E_o = 0, \quad \text{and} \quad E_{so} = 0 \quad (42)$$

This simply means that in this zone no enzyme molecule is observed either in free or immobilized form.

In the second zone,  $I_2 \equiv (X, 1]$ , the solution for the immobilized enzyme is

$$E_{so} = 1, \quad (43)$$

and the equation describing the change of intraparticle enzyme concentration is

$$\frac{1}{x^2} \frac{\partial}{\partial x} \left[ x^2 f_1(1) \frac{\partial E_o}{\partial x} \right] = 0. \quad (44)$$

Equation 44 simply means that the transport of free enzyme in the outer shell,  $I_2$ , is controlled purely by pore diffusion for which the diffusivity has been reduced by a factor of  $1/f_1(1)$ , where  $f_1(1)$  is calculated by putting  $E_s = 1$  in Eq. 19. To match consistently with the solution of the domain  $I_1$ , the boundary condition at  $x = X$  in the domain  $I_2$  is

$$x = X, \quad E_o = 0. \quad (45)$$

In order to find the exact location of the loading front  $X$ , we have to stretch the spatial variable and investigate more closely the behavior of the solution in the small neighborhood of the front. The new variable is defined as

$$\zeta = (x - X)/\mu. \quad (46)$$

Using the following expansions for  $E$  and  $E_s$ , respectively,

$$E = \mu[\bar{E}_o + 0(1)], \quad (47a)$$

$$E_s = \bar{E}_{so}. \quad (47b)$$

we obtain the following equation for the wave front position as a function of time.

$$\int_1^X \frac{X^2 \left[ \left( \frac{1}{X} - 1 \right) + \frac{f_1(1)}{Bi} \right]}{\left[ 1 + \left( \frac{\sigma}{3} \right) (X^3 - 1) \right]} dX + f_1(1) \tilde{t} = 0. \quad (48)$$

Knowing the loading front position  $X$  as a function of time (Eq. 48), the bulk enzyme concentration can be calculated from

the following equation:

$$E_b = 1 + \left(\frac{\sigma}{3}\right)(X^3 - 1), \quad (49)$$

which results from simple mass balance. It is interesting to note that the evolution of loading front and bulk enzyme concentration is independent of the Thiele modulus, (i.e.,  $K_{im}$ ) in the  $\phi \gg 1$  asymptotic regime. This is the case because the global rate of enzyme uptake by the support is controlled by the diffusion process.

### Simulation results

Computer simulation using the above model, Eqs. 32–34, has been done for different cases, including the diffusion-controlled regime, the kinetic-controlled regime, and the intermediate regime. Simulation studies were carried out with  $\phi = 1, 5, 10, 30, 50$ . The effects of different degrees of restriction have been studied for constant Thiele moduli  $\phi$ . The following parameters were employed in all the simulations:  $Bi = 500$ ,  $\psi = 0.004$ ,  $N = 0.01$ ,  $\alpha = 0.2$ .

Figures 1 and 2 show plots of  $E_s$  and  $E_b$ , respectively, for  $\phi = 1$ , indicating that the diffusional rate is relatively fast with respect to the surface coupling of enzyme. Figure 1 shows the immobilized enzyme concentration as a function of radial coordinate at various times. It is clear that the enzyme loading profile is relatively flat at any time. In this case, which is expected to result for other relatively small values of Thiele modulus (i.e.,  $\phi < 1$ ), the loading profile is always relatively uniform as diffusion resistance is very mild.

Figure 2 shows the effect of  $\phi$  on the trajectory of the enzyme concentration in the immobilizing solution. For  $\phi$  ranging between 1 and 10, the immobilizing enzyme concentration approaches the final value faster for larger  $\phi$ . A much different situation is observed when  $\phi$  is increased beyond 10.0, as discussed in the following paragraphs.

When the parameter  $\phi$  is large (i.e., more than 20), the overall immobilization process is not only dependent on the effective diffusivity of enzyme but also on the amount of enzyme loaded

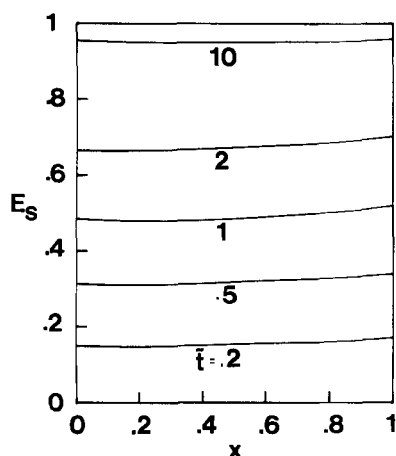


**Figure 1.** Nondimensional immobilized enzyme concentration profiles  $E_s$  at various nondimensional times  $\bar{t}$ .

$\alpha = 0.2$ ;  $\psi = 0.004$ ;  $N = 0.01$ ;  $Bi = 500$ ;  $\phi = 1.0$ .

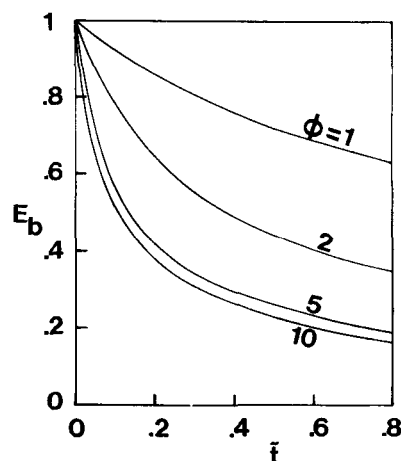


**Figure 2.** Nondimensional bulk enzyme concentration  $E_b$  vs. nondimensional time  $\bar{t}$  for different values of  $\phi$ .

$\alpha = 0.2$ ;  $\psi = 0.004$ ;  $N = 0.01$ ;  $Bi = 500$ .

into the porous support during the initial period. During this initial period, the rate of enzyme uptake is faster for larger  $\phi$ , and thus the amount of enzyme loaded is higher, Figure 3. As a consequence, the effective area for subsequent transport of enzyme into the support is reduced more for larger  $\phi$  and a slower uptake rate of enzyme for larger  $\phi$  is observed beyond the initial period; see Figure 3. However, this crossover point is dependent on the Thiele modulus value,  $\phi$ , and the degree of hindered diffusion,  $\alpha$ . Similar crossover of curves has been reported by Rajgopalan and Luss (1979) in their model predictions of demetallation rate for various pore sizes.

Figures 4 to 6 are the simulated immobilized enzyme concentration profiles for large values of  $\phi$  ( $\phi = 10, 30$ , and  $50$ ). These illustrations show that as  $\phi$  increases, the loading profile exhibits a sharper front. For very large  $\phi$  (say  $\phi = 50$ ), this front basically divides the support into two zones. The inner zone contains no enzyme in any form and the outer zone is completely saturated with immobilized enzyme. The uptake of enzyme for the case of very large  $\phi$  is controlled by the restricted diffusion of enzyme through the saturated outer shell layer, and the surface coupling of enzyme occurs mainly at the front.

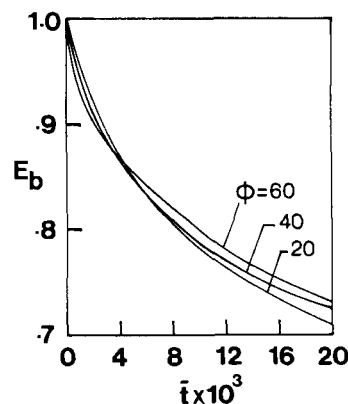


**Figure 3.** Nondimensional bulk enzyme concentration  $E_b$  vs. nondimensional time  $\bar{t}$  for high  $\phi$  values.

All other parameter values as in Figure 2.

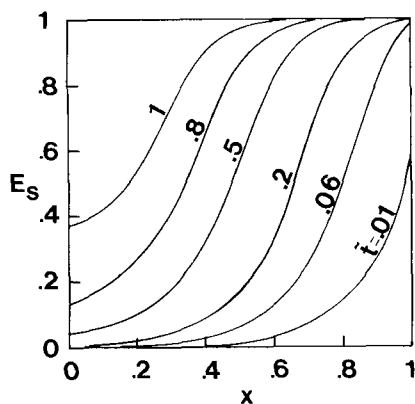


**Figure 4. Nondimensional immobilized enzyme concentration profiles  $E_s$  for various nondimensional times  $\bar{t}$ ,  $\phi = 10$ .**

All other parameter values as in Figure 2.

The effect of the degree of restriction on immobilization of enzyme has been studied and simulated; the results are plotted in Figure 7. A Thiele modulus value of 10 has been chosen as typical. The degree of restriction,  $\alpha$  (the ratio of enzyme molecule diameter to pore diameter), was varied from 0 to 0.3, all other parameters being the same. The effect of  $\alpha$  on the evolution of the reservoir enzyme concentrations is significant at high values of  $\alpha$ . The higher the value of  $\alpha$ , the greater is the restriction to diffusing enzyme molecules, reducing the rate of depletion of enzyme in the immobilizing solution. Therefore, at any given time the amount of enzyme immobilized inside the particle is lower for a larger value of  $\alpha$ . For example, after 3.0 h of contacting, the nondimensional enzyme concentration remaining in the reservoir is 0.47 for  $\alpha = 0.3$ , 0.335 for  $\alpha = 0.2$ , and 0.22 for  $\alpha = 0.0$ . In order to deplete the reservoir enzyme concentration to a value of 0.3, 2 h are required for  $\alpha = 0.0$ , while 8 h are necessary for  $\alpha = 0.3$ . This means that the restricted diffusion of enzyme molecules prolongs the immobilization process by a considerable factor.

For the diffusion-controlled regime computer simulation has been carried out using the asymptotic solutions given in Eq. 48 for the immobilized enzyme loading front position, and in Eq. 49

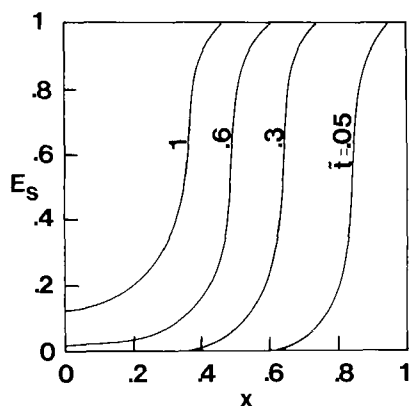


**Figure 5. Nondimensional immobilized enzyme concentration profiles  $E_s$  for various nondimensional times  $\bar{t}$ ,  $\phi = 30$ .**

All other parameter values as in Figure 2.

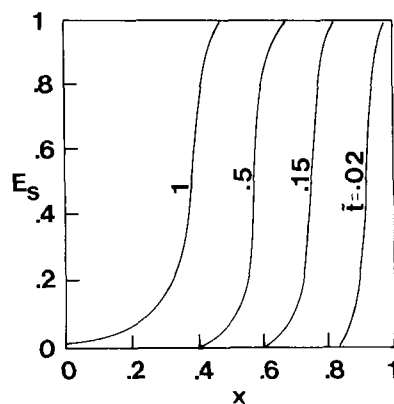


**Figure 6. Nondimensional immobilized enzyme concentration profiles  $E_s$  for various nondimensional times  $\bar{t}$ ,  $\phi = 50$ .**

All other parameter values as in Figure 2.

for the bulk enzyme concentration as a function of this front position. In these calculations, a ten-point Gaussian quadrature formula was used and the following model parameters were considered:  $Bi = 500$ ;  $\psi = 0.004$ ;  $\phi = 50$ ;  $\alpha = 0.2$ ; and  $N = 0.01$ .

Figure 8 compares the immobilized enzyme wave front position vs. time (h) obtained by collocation numerical techniques mentioned earlier with the asymptotic solution result. It is interesting to note that the time predicted by the analytical solution to achieve a certain amount of enzyme loading is slightly longer than that obtained using the numerical solution. Since the asymptotic solution has an error of  $1/\phi$ , the error associated with it is 0.02 (as  $\phi = 50$ ). Clearly, the asymptotic solution is within this range of error. This simply means that for larger values for  $\phi$ , the exact and the asymptotic results would agree better.

## Experimental

For experimental evaluation of the restricted diffusion model, the enzyme chosen was glucose oxidase and the porous support used was controlled pore glass of mesh size 80/120. The enzyme was Type V, product No. G-6500, lot No. 61F-9007 supplied by

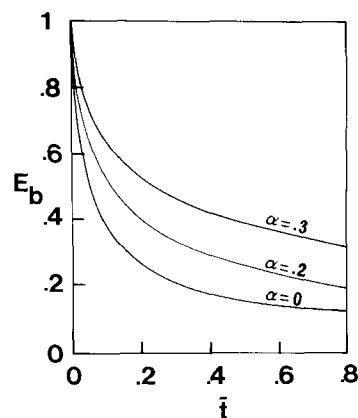


**Figure 7. Nondimensional bulk enzyme concentration  $E_b$  vs. nondimensional time  $\bar{t}$  for different values of  $\alpha$ .**

$\psi = 0.004$ ;  $N = 0.01$ ;  $Bi = 500$ .

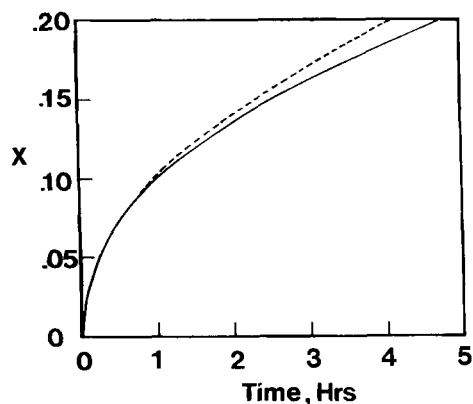


**Figure 8. Comparison of immobilized enzyme wave front position  $X$  vs. time.**

$\alpha = 0.2$ ;  $\psi = 0.004$ ;  $\phi = 50.0$ ;  $Bi = 500$ ;  $N = 0.01$ . — analytical solution; ---- numerical solution.

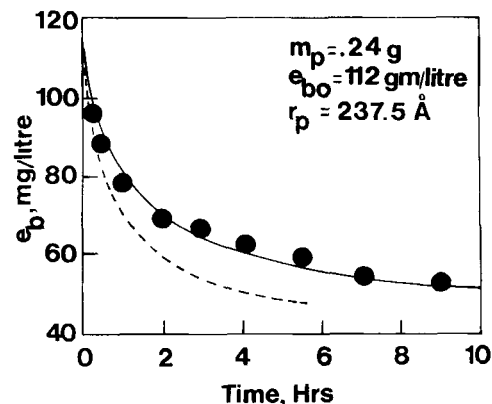


**Figure 9. ● experimental bulk enzyme concentration  $E_b$  vs. time.**

— predictions from restricted diffusion model. ---- predictions from unrestricted diffusion model.

Sigma, and the porous glass was CPG-10-500, lot No. 0045, supplied by Electronucleonics, Inc. Enzyme immobilization was carried out in a fixed-bed recirculation reactor. The immobilization technique used was silane-glutaraldehyde chemical coupling (Bouin et al., 1976). Prior to immobilization, the support was cleaned, washed, and dried. Then the support was silanized in a total reflux system with 10% solution (by volume) of  $\gamma$ -aminopropyltriethoxysilane ( $\gamma$ -APTES) in toluene (50 mL solution/g support) for 24 h. After refluxing the mixture, the support was washed with toluene five times to remove  $\gamma$ -APTES. Then it was washed with acetone to remove the toluene. The support was then allowed to air dry before placing in an oven overnight at 110°C.

Next, 25 mL of 2.5% aqueous glutaraldehyde was added to 1.0 g of silanized support for coupling reaction. The support and solution were allowed to react 30 min in vacuum and 60 min at atmospheric pressure and temperature, with occasional stirring. After decanting the glutaraldehyde, the support was washed several times to remove traces of glutaraldehyde. Meanwhile, an enzyme solution was prepared by dissolving 2 mL (5.6 mg/mL) of soluble glucose oxidase in 98 mL citrate-phosphate buffer at pH 5.5. As soon as the support was prepared, it was placed in the reactor and the enzyme coupling reaction was allowed by pumping the enzyme solution through the reactor. The protein con-

centration was measured on-line at a wavelength of 275 nm with a Varian DMS90 UV-visible spectrophotometer. The conditions of the experiment and the parameters of porous pellets are presented in Table 1. The experiment has been duplicated and the results do not vary more than  $\pm 10\%$ . Support characteristics supplied by the manufacturer have been checked by mercury porosimeter (Micromeritics model 9200) and the variation is  $\pm 5\%$ .

The resulting experimental data are plotted in Figure 9 as the bulk enzyme concentration in mg/L vs. time in h. The experimental bulk enzyme concentration levels out after 9 h of support-enzyme contacting. From this graph and using data in Table 1, the maximum immobilized enzyme concentration is 23.9 mg of protein per g of support or 16.0 mg of protein per  $\text{cm}^3$  of support. Figure 10 is a plot of the logarithm of the nondimensional bulk enzyme concentration vs. nondimensional time for an initial period of 3 min. The initial estimate of the intrinsic rate constant of immobilization as calculated from this graph is  $3.4 \times 10^{-2} \text{ cm}^3/\text{m}^2 \cdot \text{s}$  ( $\phi = 27.2$ ). The method for extracting this rate constant is described in Do and Bailey (1981). The calculated values of the parameters and constants are tabulated in Table 2. The tortuosity factor for calculating effective diffusivity has been determined experimentally by a transient desorption method (Hossain, 1985).

**Table 1. Pellet Parameters and Experimental Conditions**

Support Characteristics	
Average particle dia.	= 0.147 mm
Mean pore dia.	= 475 Å
Pore volume, $\text{cm}^3/\text{g}$	= 1.04
Surface area, $\text{m}^2/\text{g}$	= 50.7
Tortuosity*	= 2.6
Immobilization Conditions	
Vol. of enzyme solution	= 100 mL
Initial enzyme conc.	= 112 mg/L solution
Volumetric flow rate	= 48 mL/min
Mass of support	= $0.21 \pm 0.03$ g
Temperature	= $24 \pm 1^\circ\text{C}$
pH	= 5.5

\*Determined experimentally by a transient desorption method (Hossain, 1985).

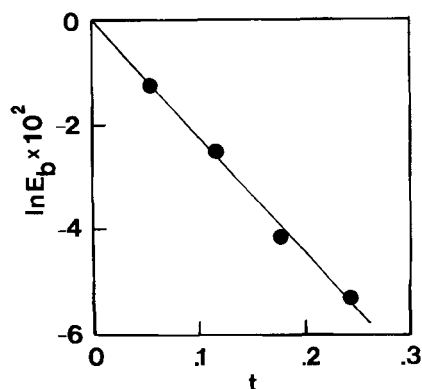


**Figure 10. Log of nondimensional bulk enzyme concentration  $E_b$  vs. nondimensional time  $t$ .**



**Table 2. Calculated Values of Parameters and Constants**

Parameter	Value	Eq. No.
$\psi = \frac{\text{Amount of enzyme in pore fluid}}{\text{Amount of enzyme on surface of support}}$	$= 4.8 \times 10^{-3}$	17 <sup>b</sup>
$N = \frac{\text{Volume of particles}}{\text{Volume of recirculating solution}}$	$= 7.0 \times 10^{-3}$	17 <sup>c</sup>
$\phi = \text{Thiele modulus (initial)}$	$= 27.2$	29
Rate constant of immobilization, $k_{im}$ (from initial rate analysis)	$= 3.4 \times 10^{-2} \text{ cm}^3/\text{m}^2 \cdot \text{s}$	17 <sup>c</sup>

The restricted diffusion model for enzyme immobilization was then solved with experimental values of various parameters, the initial estimate of the value of  $\phi$  (obtained from Figure 10), and considering the effective enzyme diameter as a varying parameter. This size of the enzyme molecule is a measure of the degree of restriction, because as the immobilization progresses more and more enzymes are loaded into the support, resulting in the reduction of diffusion area. The exact molecular size of the enzyme is not known, but the maximum dimension of the major axis is reported as 84 Å (8.4 nm). It has been found in our analyses that the computed simulation results agree more closely with the experimental data when the enzyme size is half the maximum size ( $\alpha = 0.09$ ).

A comparison between the simulation results of this model and those of the unrestricted diffusion model of Do et al. (1982b) has been made based upon the characterization of the support and the kinetic constants, the initial diffusion coefficient, and the calculated model parameters. These parameter values are used in a time-invariant sense in the unrestricted diffusion model, giving the results shown in Figure 9. In the restricted diffusion model an additional parameter, namely the effective enzyme diameter, is needed. The effective diameter employed here is reasonably related to the enzyme's maximal dimension, as just described.

Figure 11 shows the immobilized enzyme concentration profiles at various times obtained from the restricted diffusion model simulation of glucose oxidase immobilization into porous glass under these experimental conditions. The profiles are far

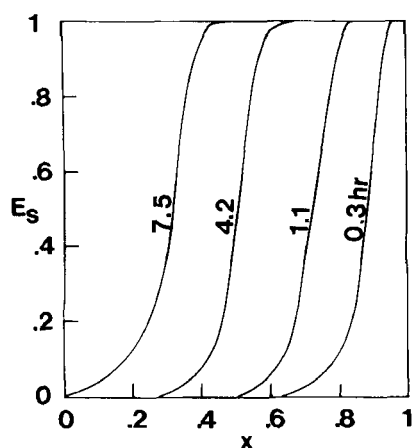


**Figure 11. Nondimensional immobilized enzyme concentration profiles  $E_s$  at various times for experimental conditions given in Tables 1 and 2.**

from uniform and exhibit a sharp front in the support. This front moves into the particle in a few hours of contacting and then the advance of the front decreases drastically as immobilization proceeds. As observed in Figure 9, the reservoir enzyme concentration depletes at a very slow rate after 5 h of enzyme-support contact. This is because of the fact that the enzymes take a much longer time to penetrate into the core of the support matrix due to severe diffusional restriction in the outer shell already saturated with immobilized enzyme. The immobilization process practically stops (i.e., reservoir enzyme concentration levels out) after 7–8 h of contact. At this time the immobilized enzyme penetration front has penetrated 65% of the support particle radius.

## Discussion

The model simulations have shown the effects of restricted diffusion of enzyme molecules within the pores on the immobilization time and the distribution of immobilized enzyme within the porous support. This also gives insights into the nature of the enzyme loading profile and its evolution with time in various controlling regimes of the immobilization process. The practical significance of the knowledge of the loading profile can be appreciated if we consider the subsequent enzymatic reaction taking place locally at the active site of immobilized enzyme.

Theoretical studies for diffusion and reaction in porous pellets done by Do and Bailey (1982), Park et al. (1981), Wang and Varma (1980), Becker and Wei (1977), and Shadman-Yazdi and Petersen (1972) have shown that the overall reaction rate is strongly influenced by the distribution of catalytic sites within the particle. The overall rate is often largest when the active site is located near the external surface rather than uniformly distributed (Wang and Varma, 1980). This conclusion has been demonstrated for immobilized enzyme catalysts as reported by Borchert and Buchholz (1979) and Dennis et al. (1984). However, from a deactivation standpoint, the work by Corbett and Luss (1974) has shown that uniformly loaded catalyst may be more stable than nonuniformly loaded catalyst. Thus there is a trade-off between nonuniform loading for high activity and uniform loading for stability (Do et al., 1982b).

From the numerical results of our restricted diffusion model, if the Thiele modulus is of the order of unity or smaller, the final enzyme loading profile is relatively uniform in both the cases of saturated and unsaturated conditions. When the Thiele modulus is relatively large ( $>5$ ), a nonuniform enzyme loading profile is obtained. The immobilized enzyme profile exhibits a relatively sharp front within the support. By choosing proper experimental conditions and conducting the immobilization experiments over a controlled period of time, the enzyme can be loaded near the external surface. This outer-shell-immobilized enzyme will subsequently yield higher activity than the uniformly distributed enzyme for the same amount of enzyme loaded as long as the enzyme-catalyzed reaction exhibits ordinary kinetics. For other kinetics, such as substrate-inhibited reactions, other intraparticle enzyme distributions may give larger overall rates (Park et al., 1981).

This model is consistent with the experimental results under the operating conditions mentioned. The model explains why the immobilization process practically stops even though the enzyme in the immobilizing bath is still available and the supports are not fully covered with immobilized enzyme. The model predictions can be used to manipulate the appropriate experimental

parameters in order to achieve a desired distribution of immobilized enzyme in the biocatalyst particles.

## Acknowledgment

The authors wish to acknowledge support for this work from the Australian Research Grant Scheme and the National Science Foundation.

## Notation

$a$  = solute radius of the diffusing molecule  
 $A$  = effective area exposed for penetration  
 $A_0$  = actual area of pore  
 $Bi$  = Biot number for mass transfer  
 $D_b$  = bulk diffusivity in free solution  
 $D_e$  = effective diffusivity, Eq. 4  
 $d_p$  = diameter of the particle  
 $c$  = intraparticle fluid enzyme concentration  
 $c_b$  = enzyme concentration in bulk (external) solution  
 $c_s$  = immobilized enzyme concentration  
 $c_{sm}$  = maximum immobilized enzyme concentration  
 $E$  = nondimensional intraparticle fluid enzyme concentration  
 $E_b$  = nondimensional bulk enzyme concentration  
 $E_s$  = nondimensional immobilized enzyme concentration  
 $E_{b0}$  = nondimensional initial bulk enzyme concentration  
 $k_{im}$  = rate constant for immobilization per unit surface area of pellet  
 $K_p$  = equilibrium partition coefficient  
 $K_r$  = fractional reduction of diffusivity of nonadsorbed solute within pores  
 $m_p$  = total mass of support  
 $N$  = ratio of supports volume to that of reservoir  
 $r$  = radial position in the pore  
 $r_p$  = radius of the particle  
 $R$  = gas law constant  
 $R_{eff}$  = effective pore radius of support particle, Eq. 7  
 $R_p$  = pore radius  
 $Sc$  = Schmidt number  
 $Sh$  = Sherwood number  
 $S_g$  = surface area of pellet per unit mass  
 $t'$  = dimensional time  
 $t$  = nondimensional time  
 $\tilde{t}$  = slow time =  $\psi t$   
 $T$  = temperature  
 $V_b$  = volume of reservoir  
 $V_{im}$  = rate of immobilization per unit available surface area of the pellet  
 $x$  = nondimensional spatial variables =  $r/r_p$   
 $X$  = enzyme loading wave front position

## Greek letters

$\alpha$  = ratio of solute molecular diameter to pore diameter  
 $\epsilon$  = pore volume fraction of support  
 $\mu$  = defined in Eq. 38  
 $\tau$  = tortuosity of the support  
 $\rho$  = solvent density  
 $\rho_p$  = density of the support particles  
 $\lambda$  = defined in Eq. 17a  
 $\phi$  = Thiele modulus  
 $\sigma$  = defined in Eq. 38  
 $\zeta$  = defined in Eq. 46  
 $\nu$  = viscosity of liquid

## Literature Cited

- Anderson, J. L., and J. A. Quinn, "Restricted Transport in Small Pores: A Model for Steric Exclusion and Hindered Particle Motion," *Bio-phys. J.*, **14**, 130 (1974).
- Bean, C. P., "The Physics of Porous Membranes—Neutral Pores," *Membranes*, G. Eiseman, ed., Dekker, New York, **1**, (1972).
- Beck, R. E., and J. S. Schultz, "Hindrance of Solute Diffusion within Membranes as Measured with Microporous Membranes of Known Pore Geometry," *Biochim. Biophys. Acta*, **255**, 273 (1972).
- Becker, E. R., and J. Wei, "Nonuniform Distribution of Catalysts on Supports," *J. Catal.*, **46**, 365 (1977).
- Bohrer, M. P., G. P. Patterson, and P. J. Carroll, "Hindered Diffusion of Dextran and Ficoll in Microporous Membranes," *Macromolecules*, **17**, 11 (1984).
- Borchert, A., and K. Buchholz, "Inhomogeneous Distribution of Fixed Enzymes inside carriers," *Biotechnol. Letters*, **1**, 15 (1979).
- Bouin, J. C., M. T. Atallah, and H. O. Hultin, "The Glucose Oxidase-Catalase System," *Methods of Enzymology*, K. Mosbach, ed., Academic Press, New York, **44**, (1976).
- Brenner, H., and L. J. Gaydos, "The Constrained Brownian Movement of Spherical Particles in Cylindrical Pores of Comparable Radius," *J. Colloid Interface Sci.*, **58**, 312 (1977).
- Brochard, F., and P. G. de Gennes, "Dynamics of Confined Polymer Chains," *J. Chem. Phys.*, **67**, 52 (1977).
- Cannell, D. S., and F. Rondelez, "Diffusion of Polystyrenes through Microporous Membranes," *Macromolecules*, **13**, 1,599 (1980); Carleysmith, S. W., M. B. L. Eames, and M. D. Lilly, "Staining Method for Determination of the Penetration of Immobilized Enzyme into a Porous Support," *Biotechnol. Bioeng.*, **22**, 957 (1980).
- Clark, D. S., J. E. Bailey, and D. D. Do, "A Mathematical Model for Restricted Diffusion Effects on Macromolecule Impregnation in Porous Supports," *Biotechnol. Bioeng.*, **27**, 208 (1985).
- Cole, J. D., *Perturbation Methods in Applied Mathematics*, Blaisdell, Waltham, MA, 13 (1968).
- Colton, D. K., C. N. Satterfield, and C. J. Lai, "Diffusion and Partitioning of Macromolecules within Finely Porous Glass," *AIChE J.*, **21**, 289 (1975).
- Corbett, W. E., and D. Luss, "The Influence of Nonuniform Catalytic Activity on the Performance of a Single Spherical Pellet," *Chem. Eng. Sci.*, **29**, 1,473 (1974).
- Daoud, M., and P. G. de Gennes, "Statistics of Macromolecular Solutions Trapped in Small Pores," *J. Physique (Paris)*, **38**, 85 (1977).
- Deen, W. M., M. P. Bohrer, and N. B. Epstein, "Effects of Molecular Size and Configuration on Diffusion in Microporous Membranes," *AIChE J.*, **27**, 952 (1981).
- de Gennes, P. G., *Scaling Concepts in Polymer Physics*, Cornell Univ. Press, Ithaca, NY (1979).
- Dennis, K. E., et al. "Immobilization of Enzymes in Porous Supports: Effects of Support-Enzyme Solution Contacting," *Biotechnol. Bioeng.*, **26**, 892 (1984).
- Do, D. D., and J. E. Bailey, "Analysis of the Initial Stages of Enzyme Immobilization in Porous Supports," *Chem. Eng. Commun.*, **12**, 221 (1981).
- , "Approximate Analytical Solutions for Porous Catalysts with Nonuniform Activity," *Chem. Eng. Sci.*, **37**, 545 (1982).
- Do, D. D., et al., "Modeling of Enzyme Immobilization," 5th Australian Biotech. Conf., Sydney (Aug., 1982a).
- Do, D. D., D. S. Clark, and J. E. Bailey, "Modeling Enzyme Immobilization in Porous Supports," *Biotechnol. Bioeng.*, **24**, (1982b).
- Do, D. D., and R. Weiland, "Deactivation of Single Catalyst Particles at Large Thiele Modulus-Travelling Wave Solutions," *Ind. Eng. Chem. Fund.*, **20**, 48 (1981).
- Ferry, J. D., "Statistical Evaluation of Sieve Constants in Ultrafiltration," *J. Gen. Physiol.*, **20**, 95 (1936).
- Hossain, Md. M., "Fundamental Studies in Enzyme Immobilization on Porous Solid Supports," M. Eng. Sci. Thesis, Univ. Queensland, St. Lucia, Qld., Australia (1985).
- Klein, E., F. F. Holland, and K. Eberle, "Comparison of Experimental and Calculated Permeability and Rejection Coefficients for Hemodialysis Membranes," *J. Membr. Sci.*, **5**, 173 (1979).
- Malone, D. M., and J. L. Anderson, "Diffusional Boundary-Layer Resistance for Membranes with Low Porosity," *AIChE J.*, **23**, 177 (1977).
- , "Hindered Diffusion of Particles through Small Pores," *Chem. Eng. Sci.*, **33**, 1,429 (1978).
- Nayfeh, A. H., *Perturbation Methods*, Wiley, New York, 110 (1973).
- Ohashi, H., et al., "Correlations of Liquid-Side Mass Transfer Coefficient for Single Particles and Fixed Beds," *J. Chem. Eng. Japan*, **14**(6), 433 (1981).
- Pappenheimer, J. R., E. M. Renkin, and L. M. Borrero, "Filtration, Diffusion and Molecular Sieving through Peripheral Capillary Membranes. A Contribution to the Pore Theory of Capillary Permeability," *Am. J. Physiol.*, **67**, 13 (1951).
- Park, S. H., S. B. Lee, and D. D. Y. Ruy, "Design of Nonuniformly Distributed Biocatalyst," *Biotechnol. Bioeng.*, **23**, 2,591 (1981).

- Rajagopalan, K., and D. Luss, "Influence of Catalyst Pore Size on Demetallation Rate," *IEC Proc. Des. Dev.*, **18**, 459 (1979).
- Renkin, E. M., "Filtration, Diffusion, and Molecular Sieving through Porous Cellulose Membranes," *J. Gen. Physiol.*, **38**, 225 (1954).
- Satterfield, C. N., C. K. Colton, and W. H. Pitcher, Jr., "Restricted Diffusion in Liquids within Fines Pores," *AIChE J.*, **19**, 628 (1973).
- Shadman-Yazdi, F., and E. E. Petersen, "Changing Catalyst Performance by Varying the Distribution of Active Catalyst with Porous Supports," *Chem. Eng. Sci.*, **27**, 227 (1972).
- Villadsen, J., and M. L. Michelsen, *Solution of Differential Equation Models by Polynomial Approximation*, Prentice-Hall, Englewood Cliffs, NJ, 143 (1978).
- Young, M. E., P. A. Carroad, and R. L. Bell, "Estimation of Diffusion Coefficients of Proteins," *Biotechnol. Bioeng.*, **22**, 942 (1980).
- Wang, J. B., and A. Varma, "On Shape Normalization for Nonuniformly Active Catalyst Pellets," *Chem. Eng. Sci.*, **35**, 613 (1980).

*Manuscript received Jan. 22, and revision received Aug. 6, 1985.*